

11-23-2007

# Stearoyl-CoA desaturase 2 is required for peroxisome proliferator-activated receptor gamma expression and adipogenesis in cultured 3T3-L1 cells

Jennifer L. Christianson

*University of Massachusetts Medical School, Jennifer.Christianson@umassmed.edu*

Sarah M. Nicoloro


*University of Massachusetts Medical School, Sarah.Nicoloro@umassmed.edu*

Juerg R. Straubhaar

*University of Massachusetts Medical School, juerg.straubhaar@umassmed.edu*

*See next page for additional authors*

Follow this and additional works at: <http://escholarship.umassmed.edu/oapubs>

 Part of the [Life Sciences Commons](#), and the [Medicine and Health Sciences Commons](#)

---

## Repository Citation

Christianson, Jennifer L.; Nicoloro, Sarah M.; Straubhaar, Juerg R.; and Czech, Michael P., "Stearoyl-CoA desaturase 2 is required for peroxisome proliferator-activated receptor gamma expression and adipogenesis in cultured 3T3-L1 cells" (2007). *Open Access Articles*. Paper 1920.

<http://escholarship.umassmed.edu/oapubs/1920>

This material is brought to you by eScholarship@UMMS. It has been accepted for inclusion in Open Access Articles by an authorized administrator of eScholarship@UMMS. For more information, please contact [Lisa.Palmer@umassmed.edu](mailto:Lisa.Palmer@umassmed.edu).

---

# Stearoyl-CoA desaturase 2 is required for peroxisome proliferator-activated receptor gamma expression and adipogenesis in cultured 3T3-L1 cells

## **Authors**

Jennifer L. Christianson, Sarah M. Nicoloso, Juerg R. Straubhaar, and Michael P. Czech

## **Rights and Permissions**

Citation: J Biol Chem. 2008 Feb 1;283(5):2906-16. Epub 2007 Nov 21. [Link to article on publisher's site](#)

# Stearoyl-CoA Desaturase 2 Is Required for Peroxisome Proliferator-activated Receptor $\gamma$ Expression and Adipogenesis in Cultured 3T3-L1 Cells<sup>\*[5]</sup>

Received for publication, July 10, 2007, and in revised form, October 26, 2007. Published, JBC Papers in Press, November 21, 2007, DOI 10.1074/jbc.M705656200

Jennifer L. Christianson, Sarah Nicoloro, Juerg Straubhaar, and Michael P. Czech<sup>1</sup>

From the Program in Molecular Medicine, University of Massachusetts Medical School, Worcester, Massachusetts 01605

Based on recent evidence that fatty acid synthase and endogenously produced fatty acid derivatives are required for adipogenesis in 3T3-L1 adipocytes, we conducted a small interfering RNA-based screen to identify other fatty acid-metabolizing enzymes that may mediate this effect. Of 24 enzymes screened, stearoyl-CoA desaturase 2 (SCD2) was found to be uniquely and absolutely required for adipogenesis. Remarkably, SCD2 also controls the maintenance of adipocyte-specific gene expression in fully differentiated 3T3-L1 adipocytes, including the expression of SCD1. Despite the high sequence similarity between SCD2 and SCD1, silencing of SCD1 did not down-regulate 3T3-L1 cell differentiation or gene expression. SCD2 mRNA expression was also uniquely elevated 44-fold in adipose tissue upon feeding mice a high fat diet, whereas SCD1 showed little response. The inhibition of adipogenesis caused by SCD2 depletion was associated with a decrease in peroxisome proliferator-activated receptor  $\gamma$  (PPAR $\gamma$ ) mRNA and protein, whereas in mature adipocytes loss of SCD2 diminished PPAR $\gamma$  protein levels, with little change in mRNA levels. In the latter case, SCD2 depletion did not change the degradation rate of PPAR $\gamma$  protein but decreased the metabolic labeling of PPAR $\gamma$  protein using [<sup>35</sup>S]methionine/cysteine, indicating protein translation was decreased. This requirement of SCD2 for optimal protein synthesis in fully differentiated adipocytes was verified by polysome profile analysis, where a shift in the mRNA to monosomes was apparent in response to SCD2 silencing. These results reveal that SCD2 is required for the induction and maintenance of PPAR $\gamma$  protein levels and adipogenesis in 3T3-L1 cells.

The ability of adipocytes to sense and respond to circulating fatty acid levels is important in maintaining the proper balance between fatty acid storage and fatty acid release for energy utilization. In the case of energy excess, fatty acids are stored in the

form of triglyceride, and new adipocytes are generated to efficiently metabolize amino acids, glucose, and fatty acids to triglyceride (1). The key regulator of adipogenesis, the process whereby preadipocytes differentiate into fully mature adipocytes, is the ligand-activated nuclear receptor PPAR $\gamma$ <sup>2</sup> (2). Cultured mouse 3T3-L1 preadipocytes are an excellent model system for the study of adipogenesis. These cells differentiate into adipocytes with multilocular lipid droplets through a transcriptional cascade beginning with the rapid and transient expression of C/EBP $\beta$  and C/EBP $\delta$  (3, 4). The up-regulation of these transcription factors precedes the expression of PPAR $\gamma$  and C/EBP $\alpha$ , which are critical for the completion of adipogenesis as well as the maintenance of adipocyte-specific gene expression in fully differentiated cells (3, 4). Other transcription factors have also been shown to play significant roles in adipogenesis and adipocyte biology (for reviews, see Refs. 3, 5, and 6). However, because PPAR $\gamma$  controls the expression of large sets of genes required to maintain the adipocyte phenotype, including C/EBP $\alpha$  itself, a loss in the activity or expression of PPAR $\gamma$  leads to a loss in adipocyte function (7).

Although it is unclear whether ligands actively modulate PPAR $\gamma$  activity in fully differentiated adipocytes, ligand-mediated activation of PPAR $\gamma$  appears to be required for transcriptional activity during adipogenesis (8). Because PPAR $\gamma$  has a large hydrophobic ligand binding domain (9) and activation occurs in response to fatty acids (10), endogenous long chain fatty acids or their derivatives have been proposed as natural ligands. These include oleate, linoleate, nitrolinoleate, nitro-oleate, 9-hydroxydecaenoic acid, arachidonic acid, and 15-deoxy-prostaglandin J<sub>2</sub> (11–15). Despite the many proposed ligands, nitrolinoleate and nitro-oleate are the only fatty acids with a high binding affinity, but it has not yet been verified that these fatty acids are truly endogenous PPAR $\gamma$  ligands in adipocytes (13, 15). Because several low affinity fatty acid ligands activate PPAR $\gamma$  (11–13, 16, 17), this nuclear receptor may

\* This work was supported by National Institutes of Health Grant DK30898, the Genomics and Bioinformatics Core Facilities of the University of Massachusetts Diabetes and Endocrinology Center (National Institutes of Health Grant DK32520), and the Diabetes Genome Anatomy Project (National Institutes of Health Grant DK60837). The costs of publication of this article were defrayed in part by the payment of page charges. This article must therefore be hereby marked "advertisement" in accordance with 18 U.S.C. Section 1734 solely to indicate this fact.

[5] The on-line version of this article (available at <http://www.jbc.org>) contains supplemental Figs. 1 and 2 and Table 1.

<sup>1</sup> To whom correspondence should be addressed: Program in Molecular Medicine, University of Massachusetts Medical School, 373 Plantation St., Suite 100, Worcester, MA 01605. Tel.: 508-856-2254; Fax: 508-856-1617; E-mail: Michael.Czech@umassmed.edu.

<sup>2</sup> The abbreviations used are: PPAR $\gamma$ , peroxisome proliferator-activated receptor  $\gamma$ ; SCD1–5, stearoyl-CoA desaturase 1–5; C/EBP $\beta$ ,  $\delta$ , or  $\alpha$ , CCAAT/enhancer-binding protein  $\beta$ ,  $\delta$ , or  $\alpha$ ; GLUT4, insulin-responsive facilitated glucose transporter isoform 4; ACC $\beta$ , acetyl-coenzyme A carboxylase  $\beta$ ; FAS, fatty acid synthase; AKT1, thymoma viral proto-oncogene 1; PTEN, phosphatase and tensin homolog; mTOR, mammalian target of rapamycin; RS6K1/2, 40 S ribosomal protein S6 kinase 1/2; eEF2, eukaryotic translation elongation factor 2; eEF2K, eEF 2 kinase; eIF2 $\alpha$ , eukaryotic translation initiation factor 2 $\alpha$ ; siRNA, small interfering RNA; SREBP1, sterol regulatory element-binding protein-1; MTS, 3-(4,5-dimethylthiazol-2-yl)-5-(3-carboxymethoxyphenyl)-2-(4-sulfophenyl)-2H-tetrazolium; PBS, phosphate-buffered saline.

instead serve as a general fatty acid sensor, allowing proper expression of fatty acid metabolizing enzymes and the generation of new adipocytes.

In addition, it appears that differentiating adipocytes can fully synthesize a PPAR $\gamma$  ligand, since preadipocytes will differentiate and produce a PPAR $\gamma$  ligand in the absence of exogenous fatty acids (14, 18). Furthermore, overexpression of sterol regulatory element-binding protein-1 (SREBP1) in adipocytes apparently increases ligand production (19), whereas inhibition of acetyl-CoA carboxylase (ACC) (20) or fatty acid synthase (FAS) (21) inhibits adipogenesis. SREBP1 is a transcription factor that controls the expression of many fatty acid metabolizing enzymes, including ACC and FAS. Because ACC and FAS work sequentially to produce palmitate, it is possible that sterol regulatory element-binding protein-1 promotes PPAR $\gamma$  ligand production through a pathway involving ACC and FAS. Although there may be several explanations for the requirement of SREBP1, ACC, or FAS for adipogenesis apart from PPAR $\gamma$  ligand production, these studies do support the notion that endogenously synthesized fatty acids are required for adipogenesis.

Because adipocytes express multiple fatty acid-metabolizing enzymes, these cells apparently produce highly diverse lipid species that may affect cellular signaling events, including PPAR $\gamma$  activation. Thus, the aim of the present study was to identify enzymes involved in fatty acid synthesis or metabolism that may mediate such signaling pathways through their fatty acid products. To achieve this goal, we set up a screen in which 24 fatty acid-metabolizing enzymes were individually depleted using siRNA oligonucleotides to identify enzymes that are required for adipocyte-specific gene expression. Through this siRNA screen, we identified the fatty acid  $\Delta$ 9-desaturase, stearoyl-CoA desaturase 2 (SCD2), as a required enzyme for 3T3-L1 cell adipogenesis and for the maintenance of adipocyte-specific gene expression in fully differentiated cells. Importantly, SCD2 was found to be required for PPAR $\gamma$  induction during differentiation of 3T3-L1 cells and for PPAR $\gamma$  expression in fully differentiated adipocytes. Related to this latter effect, SCD2 expression was found to promote protein translation, secondarily affecting PPAR $\gamma$  protein levels. Surprisingly, although SCD1 and SCD2 exhibit high sequence similarity, are both expressed in the endoplasmic reticulum of the adipocyte, and are predicted to produce the same products, SCD1 depletion failed to attenuate PPAR $\gamma$  expression or adipogenesis. Therefore, these results identify SCD2 as a key regulator of adipocyte function by promoting PPAR $\gamma$  protein synthesis and reveal a novel and specific role for SCD2 *versus* SCD1 in the adipocyte.

## EXPERIMENTAL PROCEDURES

**Animals**—All procedures were carried out following the University of Massachusetts Medical School Institution Animal Care and Use Committee guidelines. Four-week-old male C57BL/6J mice were purchased from The Jackson Laboratory (Bar Harbor, ME) and maintained in a 12-h light/dark cycle. Half of the mice were fed a standard mouse chow (10% kcal of fat), and the other half was fed a high fat diet (55% kcal of fat) *ad libitum* for 18 weeks. The animals were fasted for 18 h before harvesting the tissues. Animals were sacrificed, epididymal fat

pads were harvested from the mice and placed in KRH buffer (pH 7.4) supplemented with 2.5% bovine serum albumin, and RNA was collected using TRIzol (Invitrogen) for subsequent Affymetrix GeneChip analysis.

**Materials**—Rosiglitazone was purchased from Biomol (Plymouth Meeting, PA). The proteasome inhibitor, MG132, was purchased from Calbiochem. Mouse monoclonal anti-PPAR $\gamma$ , mouse monoclonal anti-AKT1, mouse monoclonal anti- $\beta$  catenin, rabbit polyclonal anti-PPAR $\gamma$ , and rabbit polyclonal anti-C/EBP $\alpha$  antibodies were purchased from Santa Cruz Biotechnology. Rabbit anti-AMP-activated protein kinase, eEF2, RS6K, and eIF2 $\alpha$  were purchased from Cell Signaling (Danvers, MA). Protein A-Sepharose beads were purchased from Sigma. Rabbit PTEN antiserum was purchased from Upstate Biotechnology (Charlottesville, VA). The MTS (3-(4,5-dimethylthiazol-2-yl)-5-(3-carboxymethoxyphenyl)-2-(4-sulfophenyl)-2H-tetrazolium) cell proliferation assay kit and TdT-mediated dUTP nick-end labeling kit were purchased from Promega (Madison, WI). The iScript cDNA synthesis kit and the iQ SYBR green supermix kit were purchased from Bio-Rad. [<sup>35</sup>S]Methionine/cysteine was purchased from PerkinElmer Life Sciences.

**siRNA Duplexes**—The siRNA purchased from Dharmacon Inc. (Lafayette, CO) were designed to target the following cDNA sequences: scrambled, 5'-CAGTCGCGTTTGCGACTGG-3'; SCD2, 5'-GAGCAGATGTTCCGCCCTGATT-3'; PPAR $\gamma$ , 5'-GACATGAATTCCTTAATGA-3'; SCD1, 5'-GCCTAGAAC-TGATAACTAATT-3'. Proprietary SMART-pool siRNA duplexes were used to target all other transcripts.

**Cell Culture and Electroporation**—3T3-L1 fibroblasts were cultured in Dulbecco's modified Eagle's medium supplemented with 10% fetal bovine serum, 50  $\mu$ g/ml streptomycin, and 50 units/ml penicillin (22). For experiments performed during differentiation, fibroblasts were cultured for 7 days, and  $5 \times 10^6$  cells were electroporated with 20 nmol of siRNA. The electroporation was performed using a Bio-Rad Gene Pulser II at the setting of 0.18 kV and 960 microfarads. Immediately after electroporation, the cells were reseeded into 2 wells of a 6-well plate. After 24 h, differentiation media consisting of 2.5  $\mu$ g/ml insulin, 0.25  $\mu$ M dexamethasone, and 0.5 mM 3-isobutyl-1-methyl-xanthine in the culture media described above was added for 72 h in the absence or presence of 1  $\mu$ M rosiglitazone. After 72 h, differentiation media was replaced with culture media for an additional 24 h, and then RNA or protein was collected. For experiments in mature adipocytes, fibroblasts were cultured for 8 days, differentiated into mature adipocytes as described above, and cultured for an additional 7 days. Adipocytes were then electroporated (20 nmol of siRNA/ $5 \times 10^6$  cells) as described above. After electroporation, cells were reseeded into multiple-well plates, and RNA or protein was collected 4–72 h post-electroporation.

**Affymetrix Gene Chip Analysis**—Total RNA was collected from day 10 adipocytes after 72 h of siRNA treatment or from preadipocyte fibroblasts, adipocytes, and primary fat tissue as described (23). Subsequent reactions were carried out as already described (24). Only signals considered present were used for further analysis. If more than one probe is present, only one representative probe is shown.

## Regulation of PPAR $\gamma$ Expression by SCD2

**RNA Isolation and Real Time-PCR**—Total RNA was collected using TRIzol (Invitrogen), and reverse transcription and real time-PCR analysis were carried out as already described (24, 50). Primers were chosen from the PrimerBank online data base (25). AKT1 was used as the internal control.

**Immunoblotting**—Cells were solubilized with lysis buffer containing 25 mM Hepes (pH 7.5), 0.5% Nonidet P-40, 1 mM EGTA, 1 mM EDTA, 1% SDS, 12.5 mM NaF, 5 mM sodium pyrophosphate, 5 mM  $\beta$ -glycerophosphate, 5 mM sodium vanadate, 1 mM phenylmethylsulfonyl fluoride, 5  $\mu$ g/ml aprotinin, and 10  $\mu$ g/ml leupeptin. Protein was quantified using the BCA protein assay kit (Pierce) and then resolved on a 8% SDS-PAGE gel, electrotransferred to nitrocellulose, blocked with 5% bovine serum albumin and 5% nonfat milk in TBST (0.05% Tween 20 in Tris-buffered saline), washed with TBST, and incubated with specific antibody at 4 °C overnight. The blots were then washed with TBST, and a horseradish peroxidase anti-mouse or anti-rabbit secondary antibody was applied. Proteins were visualized using an enhanced chemiluminescent substrate kit (Amersham Biosciences), and immunoblot band intensities were quantified by scanning densitometry using Photoshop.

**Oil Red O Staining**—Cells were fixed with 4% formaldehyde for 1 h at room temperature, washed 3 times with PBS, permeabilized with P-buffer (0.5% Triton X-100, 1% fetal bovine serum, and 0.05% sodium azide) for 20 min, incubated with Oil Red O solution (5 mg/ml Oil Red O solid dissolved in isopropanol then diluted to a 60% working solution with double-distilled H<sub>2</sub>O) for 30 min, washed 3 times with distilled water, and analyzed by light microscopy or visual inspection.

**[<sup>35</sup>S]Methionine/Cysteine Labeling and Immunoprecipitation of PPAR $\gamma$** —Seventy-two hours after electroporation of cells with siRNA, one 100-mm plate of cells was starved of methionine and cysteine for 2 h and then labeled with 500  $\mu$ Ci of [<sup>35</sup>S]methionine/cysteine for 4 h. Cells were then lysed in ice-cold buffer containing 25 mM Hepes (pH 7.5), 0.5% Nonidet P-40, 1 mM EGTA, 1 mM EDTA, 1% SDS, 12.5 mM NaF, 5 mM sodium pyrophosphate, 5 mM  $\beta$ -glycerophosphate, 5 mM sodium vanadate, 1 mM phenylmethylsulfonyl fluoride, 5  $\mu$ g/ml aprotinin, and 10  $\mu$ g/ml leupeptin. Total cell lysates of 1 mg of protein were immunoprecipitated overnight with 20  $\mu$ g of mouse monoclonal antibody against PPAR $\gamma$  followed by incubation with 50  $\mu$ l of protein A-Sepharose beads for 2 h at 4 °C. The beads were then washed 5 times with lysis buffer before boiling for 5 min in Laemmli buffer. Protein was then separated on an 8% SDS gel, transferred to nitrocellulose, and exposed to a phosphor screen for 60 h. The screen was then visualized with a PhosphorImager (Molecular Dynamics). The nitrocellulose was then immunoblotted as described above using goat polyclonal antibody against PPAR $\gamma$  to detect the efficiency of the immunoprecipitation.

**Polysome Profile and Reverse Transcription-PCR**—Polysome profiles were generated as described previously (26–28). Briefly, after siRNA transfection, cells were reseeded into one 10-cm dish. After 24 or 72 h, cycloheximide (Sigma) was added at a final concentration of 100 mg/ml for 10 min. Cells were then washed with PBS, trypsinized, pelleted, and resuspended in polysome buffer (20 mM Tris-HCl (pH 7.5), 10 mM NaCl, 3 mM MgCl<sub>2</sub>) containing 150  $\mu$ g/ml cycloheximide and 100

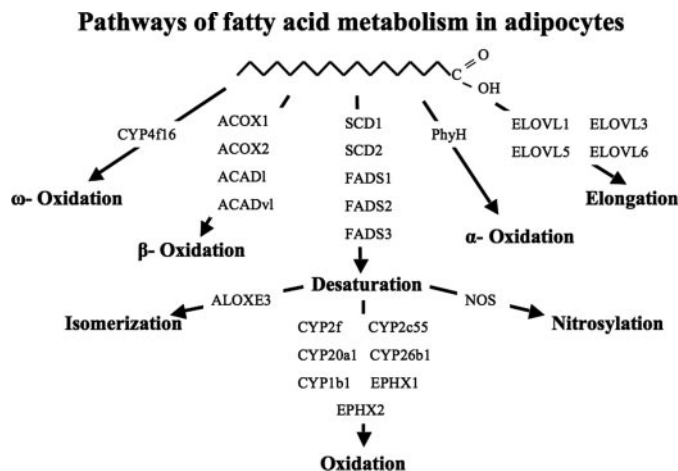


**FIGURE 1. Diagram showing the multiple pathways of fatty acid metabolism in adipocytes.** A saturated fatty acid may be  $\omega$ -oxidized, forming a dicarboxylic acid;  $\beta$ -oxidized, cleaving two carbons per cycle from the fatty acid;  $\alpha$ -oxidized, cleaving one carbon per cycle from the fatty acid; Elongated, adding two carbons per cycle to the fatty acid; Desaturated, forming a cis-double bond between the 9 and 10, 5 and 6, 6 and 7, or possibly the 4 and 5 carbons. The double bond in a desaturated fatty acid may then change position through isomerases or be nitrated or oxidized, producing various side groups on the fatty acid (see under "Results" for further details). EPHX, epoxide hydrolase; ACOX, acyl-CoA oxidase.

units/ml RNasin (Promega). After determining the cell number in each sample, Triton X-100 was added to the cell suspension at a final concentration of 0.3% (v/v), and cells were passed through a 27-gauge needle 5 times to ensure lysis. The nuclei were then pelleted by centrifugation at 4 °C and 12,000  $\times$  g for 5 min. The supernatant was then layered on a linear 10–50% sucrose gradient in polysome buffer containing 10  $\mu$ g/ml cycloheximide and 3.3 units/ml RNasin, and the gradients were centrifuged in a Beckmann SW41Ti Rotor at 141,000  $\times$  g at 4 °C for 4 h. The gradients were fractionated into 1-ml fractions, and the UV absorption at A254 was recorded. Twelve fractions were collected, and RNA was then extracted from each fraction using TRIzol (Invitrogen). Equal volumes of each fraction were then reverse-transcribed, and real time PCR was performed as already described (24).

## RESULTS

**Expression of Fatty Acid Metabolizing Enzymes in Cultured Adipocytes and Primary Adipose Tissue**—To establish a siRNA-based screen of broad scope, we first identified key enzymes in the major pathways of fatty acid metabolism that are clearly expressed in both mouse 3T3-L1 adipocytes and primary mouse adipose tissue. Fig. 1 illustrates eight pathways of fatty acid metabolism that were considered for our studies, which include  $\omega$ -oxidation,  $\beta$ -oxidation,  $\alpha$ -oxidation, elongation, desaturation, nitration, epoxygenation/hydroxylation, and isomerization. Identification of the enzymes shown in Fig. 1 was accomplished by Affymetrix GeneChip microarray analysis of samples obtained from 3T3-L1 preadipocytes versus 3T3-L1 adipocytes (6 days after initiation of differentiation) and from the adipose tissue of mice fed a normal diet versus a high fat diet for 16 weeks. Table 1 presents the list of specific genes we selected by this analysis, all of which were found to be significantly expressed in both model systems. Boldface shows values

TABLE 1

Affymetrix Gene Chip analysis of fatty acid metabolizing enzymes in differentiating 3T3-L1 adipocytes and primary adipocytes from mice fed a normal chow or high fat diet

RNA was collected from 3T3-L1 cells before differentiation or 2, 4, and 6 days post-differentiation and subjected to Affymetrix Gene Chip analysis. RNA from three different samples was collected and pooled and then analyzed on one array; each experiment was done in triplicate, resulting in a total of nine RNA samples and three arrays for each timepoint. From the primary adipocytes, RNA was collected from 23 mice fed a normal chow diet and 14 mice fed a high fat diet for 18 weeks. The mice were divided into three groups within each diet condition, and the RNA from each group was pooled and then analyzed on one array, resulting in three arrays for each diet condition. Shown are representative values for the -fold changes in gene expression during adipogenesis or due to high fat diet. Boldface shows values that are significantly up-regulated or down-regulated in response to 3T3-L1 differentiation. The values obtained for SCD1 and SCD2 are in the rectangle. The asterisk denotes a *p* value <0.05.

| Gene Symbol   | 3T3-L1 adipogenesis (fold change) | <i>P</i> value | chow fed vs high fat diet (fold change) | <i>P</i> value |
|---------------|-----------------------------------|----------------|---|----------------|
| Ppar $\gamma$ | <b>5.28</b>                       | <b>0.047*</b>  | <b>-1.68</b>                            | <b>0.011*</b>  |
| Fasn          | <b>5.83</b>                       | <b>0.003*</b>  | <b>2.96</b>                             | <b>0.021*</b>  |
| Scd1          | <b>35.23</b>                      | <b>0.009*</b>  | <b>1.25</b>                             | <b>0.044*</b>  |
| Scd2          | <b>2.96</b>                       | <b>0.009*</b>  | <b>44.06</b>                            | <b>0.000*</b>  |
| Fads1         | 1.89                              | 0.110          | 1.17                                    | 0.276          |
| Fads2         | 2.31                              | 0.170          | 2.13                                    | 0.002          |
| Fads3         | 1.98                              | 0.182          | 1.95                                    | 0.001          |
| Elov11        | 1.04                              | 0.847          | 1.46                                    | 0.005          |
| Elov12        | 1.03                              | 0.622          | -1.02                                   | 0.690          |
| Elov13        | <b>6.36</b>                       | <b>0.004*</b>  | <b>2.07</b>                             | <b>0.009*</b>  |
| Elov14        | 1.05                              | 0.471          | -1.02                                   | 0.603          |
| Elov15        | 1.21                              | 0.354          | 1.62                                    | 0.006          |
| Elov16        | -1.76                             | 0.075          | 5.08                                    | 0.010          |
| Acadvl        | <b>4.13</b>                       | <b>0.001*</b>  | 1.18                                    | 0.241          |
| Acadl         | <b>2.78</b>                       | <b>0.001*</b>  | <b>1.33</b>                             | <b>0.016*</b>  |
| Acox1         | <b>4.60</b>                       | <b>0.000*</b>  | 1.07                                    | 0.520          |
| Acox2         | <b>5.94</b>                       | <b>0.011*</b>  | 1.13                                    | 0.540          |
| Acox3         | <b>2.10</b>                       | <b>0.002*</b>  | 1.13                                    | 0.200          |
| Ephx1         | 1.14                              | 0.856          | 2.94                                    | 0.006*         |
| Ephx2         | <b>3.43</b>                       | <b>0.003*</b>  | <b>1.22</b>                             | <b>0.025*</b>  |
| Nos3          | <b>2.05</b>                       | <b>0.010*</b>  | <b>1.48</b>                             | <b>0.029*</b>  |
| Cyp2f2        | <b>5.73</b>                       | <b>0.011*</b>  | <b>-2.91</b>                            | <b>0.024*</b>  |
| Cyp2e55       | <b>-1.68</b>                      | <b>0.049*</b>  | 1.00                                    | 0.960          |
| Cyp4f16       | -1.41                             | 0.078          | 1.07                                    | 0.539          |
| Cyp20a1       | 1.04                              | 0.795          | -1.04                                   | 0.781          |
| Cyp1b1        | -2.38                             | 0.093          | -2.85                                   | 0.012*         |
| Cyp51         | <b>5.82</b>                       | <b>0.007*</b>  | <b>4.08</b>                             | <b>0.000*</b>  |
| Aloxe3        | 1.08                              | 0.356          | 1.07                                    | 0.489          |

for -fold change in expression for genes that are significantly up-regulated or down-regulated in response to 3T3-L1 differentiation (Table 1). The values obtained for SCD1 and SCD2 are highlighted within the rectangle.

The fatty acid-metabolizing enzymes shown in Table 1 and Fig. 1 allow the generation of many different fatty acid products and derivatives from the same initial fatty acid substrate. A saturated fatty acid such as palmitate may be 1)  $\omega$ -oxidized by the cytochrome P450 enzyme CYP4f16, forming a dicarboxylic acid, 2)  $\beta$ -oxidized in peroxisomes by the acyl-CoA oxidases ACOX1 and ACOX2 or in the mitochondria by the acyl-CoA dehydrogenases ACADL and ACADVL, cleaving two carbons per cycle from the fatty acid, 3)  $\alpha$ -oxidized in peroxisomes by phytanoyl-CoA hydroxylase, cleaving one carbon per cycle from the fatty acid, 4) elongated by ELOVL1, ELOVL3, ELOVL5, and ELOVL6, which are present in the endoplasmic reticulum, adding two carbons per cycle to the fatty acid, or 5) desaturated by various enzymes found in the endoplasmic reticulum, including stearoyl-CoA desaturase 1 or stearoyl-

CoA desaturase 2, forming a cis double bond between the 9 and 10 carbons, or fatty acid desaturase 1, fatty acid desaturase 2, or fatty acid desaturase 3, forming a cis double bond between 5 and 6, 6 and 7, and possibly the 4 and 5 carbons, respectively. In addition, the double bond in an unsaturated fatty acid may change position through the isomerase, ALOXE3, found in the cytoplasm, be nitrated by nitric oxide species produced by nitric-oxide synthase, found in the cytoplasm, or be oxidized by the cytochrome P450 enzymes CYP2f2, CYP2c55, CYP20a1, CYP26b1, CYP1b1, found in the endoplasmic reticulum, adding an epoxide, hydroxyl, or peroxy group to the fatty acid. An epoxide may then be further metabolized by the epoxide hydrolase, EPHX1, present in the endoplasmic reticulum, or EPHX2, present in the cytoplasm, producing dihydrodiols. Additionally, these pathways can operate in tandem, changing the carbon length or position of a side group or double bond within the fatty acid. Because a fatty acid produced from any one of these pathways may affect cell signaling events or other processes, these enzymes listed in Table 1 were targeted in a siRNA-based screen to determine whether they affect adipocyte gene expression in 3T3-L1 cells.

*SCD2, but Not SCD1, Is Required for 3T3-L1 Adipogenesis*—To identify fatty acid metabolizing enzymes that are required for 3T3-L1 adipogenesis, siRNA oligonucleotides directed against each of the enzymes identified by the microarray analysis in Table 1 were electroporated into 3T3-L1 preadipocytes before differentiation. Because PPAR $\gamma$  appears to be activated by an endogenous ligand during adipogenesis (8, 11–13, 16), we reasoned that if a depleted enzyme is required specifically for the production of a PPAR $\gamma$  ligand, the addition of an exogenous ligand may reverse the effect of such enzyme depletion. Thus, in our screen the enzymes were also depleted in the presence of the PPAR $\gamma$  specific ligand, rosiglitazone, as a control. The initial screen monitored the mRNA transcript levels by real time PCR of the differentiation-induced proteins PPAR $\gamma$  and GLUT4 (Fig. 2). As expected, the well established required factors for adipocyte differentiation, PPAR $\gamma$  and FAS (21), did indeed attenuate PPAR $\gamma$  and GLUT4 expression in this screen when depleted by siRNA and acted as positive controls. In addition, rosiglitazone treatment did not restore PPAR $\gamma$  or GLUT4 levels upon siRNA-based depletion of PPAR $\gamma$  (Fig. 2 and supplemental Fig. 1). Importantly, of the remaining 24 enzymes screened, only SCD2 depletion potentially inhibited gene expression during adipogenesis (Fig. 2, A and B).

Interestingly, despite the predicted similarity in substrate selectivity between SCD1 and SCD2 (29), depletion of SCD1 in 3T3-L1 cells did not inhibit PPAR $\gamma$  or GLUT4 expression (Figs. 2 and supplemental Fig. 1). Furthermore, the addition of rosiglitazone did not restore the transcript levels of PPAR $\gamma$  or GLUT4 upon loss of SCD2 or FAS (Fig. 2 and supplemental Fig. 1). This suggests that if SCD2 and FAS are involved in PPAR $\gamma$  ligand production during adipogenesis, the enzymes are also required for an independent function.

In an attempt to confirm and extend these findings, expression of PPAR $\gamma$  protein was measured in a second screen of 10 enzymes, again revealing that SCD2, but not SCD1, is abso-

## Regulation of PPAR $\gamma$ Expression by SCD2

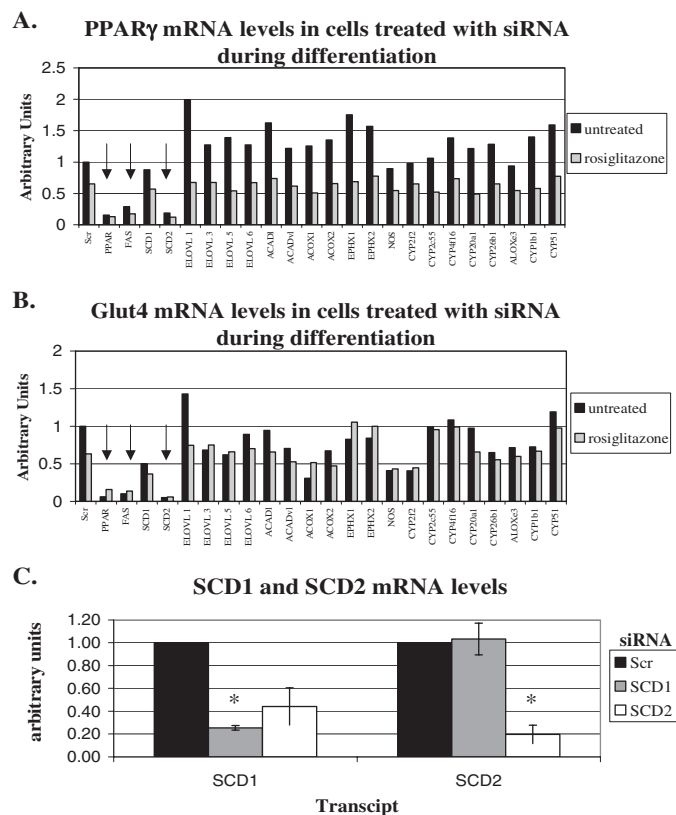


**FIGURE 2. Depletion of SCD2 inhibits the mRNA expression of adipogenic markers in differentiating 3T3-L1 adipocytes.** Confluent fibroblasts were electroporated with scrambled nucleotide as a control or SMART-pool siRNA directed against various fatty acid metabolizing enzymes and reseeded in duplicate wells as described under "Experimental Procedures." After 24 h, the cells were differentiated in the presence or absence of 1  $\mu$ M rosiglitazone. On the fourth day of differentiation, RNA was collected to determine the expression of PPAR $\gamma$  (A), GLUT4 (B), or SCD1 and SCD2 (C) by real time PCR using AKT1 as an internal control. The results shown in A and B were performed once as part of the initial screen; the results shown in C are an average of three independent experiments, and the asterisk denotes a *p* value < 0.01. EPHX, epoxide hydrolase; ACOX, acyl-CoA oxidase; NOS, nitric-oxide synthase.

lutely required for expression of this transcription factor (Fig. 3A). In addition, when preadipocytes differentiate into adipocytes, the cells become smaller and rounder, losing their fibroblastic morphology. The cells also acquire the ability to accumulate lipid in the form of triglyceride, appearing as lipid droplets in the cytoplasm (3, 14). Oil Red O staining of accumulated neutral lipids in cells 4 days after the initiation of differentiation confirms that PPAR $\gamma$  and SCD2 are required for the lipid accumulation (Fig. 3B) and morphological changes (data not shown) that occur during adipogenesis, whereas SCD1 is not. Therefore, SCD2, but not SCD1, is required for several aspects of adipogenesis, including the induction of adipocyte specific genes, the increase in lipid accumulation, and the gain in the adipocyte morphology.

To verify that the inhibition of adipogenesis by depletion of PPAR $\gamma$ , FAS, or SCD2 is not due to general toxicity, metabolic activity was measured in the cells using the tetrazolium compound, MTS. MTS is reduced by the cells to a colored formazan product, presumably by NADPH or NADH produced by dehydrogenase enzymes, and therefore, is an indirect measure of dehydrogenase activity. As seen in Fig. 4A, depletion of the various PPAR $\gamma$ zymes using siRNA did not cause a reduction in

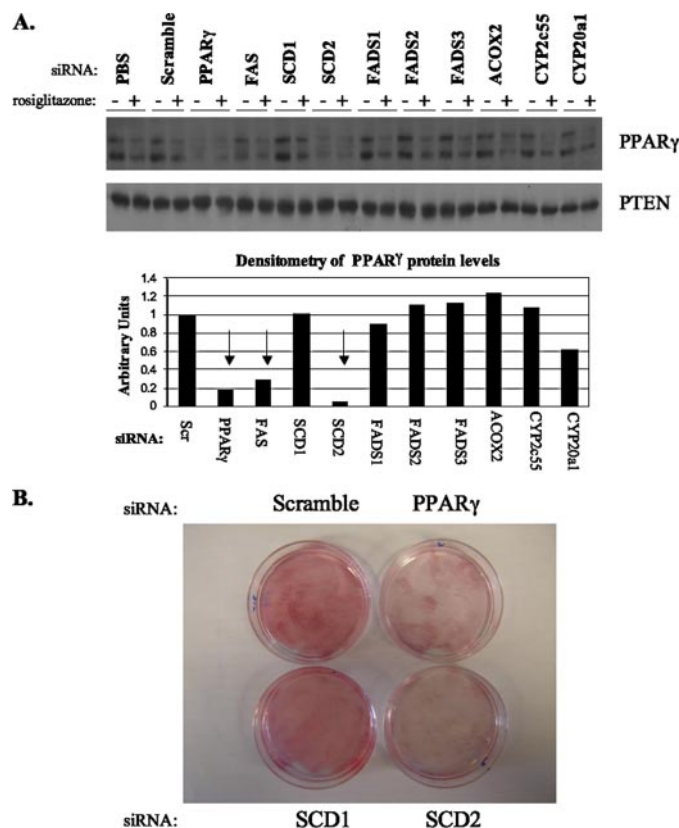


**FIGURE 3. Depletion of SCD2 inhibits adipogenic protein expression and morphological changes in differentiating 3T3-L1 adipocytes.** Confluent fibroblasts were electroporated with scrambled nucleotide as a control or SMART-pool siRNA directed against various fatty acid metabolizing enzymes and reseeded in duplicate wells as described under "Experimental Procedures." After 24 h the cells were differentiated in the presence or absence of 1  $\mu$ M rosiglitazone. On the fourth day of differentiation protein was collected to determine the expression of PPAR $\gamma$  by Western blot using PTEN as a loading control; densitometry values reflect the ratio of PPAR $\gamma$  to PTEN (A). B, cells were electroporated and differentiated as described in A, then fixed and stained with Oil Red O 4 days post-differentiation. ACOX, acyl-CoA oxidase.

dehydrogenase activity, and therefore, the inhibition of adipogenesis does not appear to be due to general toxicity. We also found an increase in the expression of several caspases with SCD2 depletion (supplemental Table 1). Because caspases are involved in apoptosis, a TdT-mediated dUTP nick-end labeling assay was performed to ensure that the siRNA treatment does not induce apoptosis. This assay utilizes fluorescein-12-dUTP and terminal deoxynucleotidyltransferase to fluorescently label the fragmented DNA of apoptotic cells on the free 3'OH DNA ends. The fluorescence of the cell population is then quantitated by flow cytometry to determine the extent of apoptosis occurring within the cell population. As can be seen in Fig. 4B, depletion of PPAR $\gamma$ , FAS, SCD1, or SCD2 does not induce apoptosis, and therefore, the effects on gene expression are not due to this toxic event.

**SCD2, but Not SCD1, Is Required for Adipocyte-specific Gene Expression in Fully Differentiated Adipocytes**—Real time PCR analysis reveals that SCD2 expression is higher in preadipocyte fibroblasts than SCD1 expression (supplemental Fig. 2, A and C), but 6 days after the induction of differentiation, SCD1 expression increases by 23-fold (supplemental Fig. 2B), whereas SCD2 expression only increases by ~8-fold (supplemental Fig.

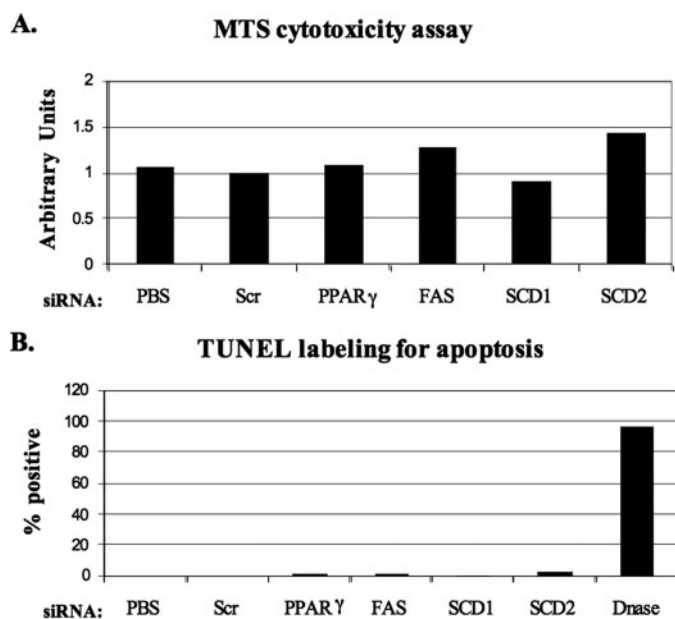


**FIGURE 4. The treatment of cultured 3T3-L1 cells with siRNA does not induce toxicity.** *A*, confluent 3T3-L1 fibroblasts were transfected with PBS or scrambled nucleotide as controls or SMART-pool siRNA against PPAR $\gamma$ , FAS, SCD1, or SCD2 transcript and differentiated as described. Toxicity was then determined using the colorimetric MTS cell proliferation assay (Promega). *B*, seven days post-differentiation, adipocytes were electroporated with PBS or scrambled nucleotide as controls or siRNA against PPAR $\gamma$ , FAS, SCD1, or SCD2 transcript. After 72 h, the cells were labeled for apoptosis using the TdT-mediated dUTP nick-end labeling (TUNEL) assay kit (Promega), and positively labeled cells were determined by FACS analysis. DNase-treated cells acted as the positive control.

2, *B* and *C*). This dramatic induction of SCD1 expression results in higher SCD1 than SCD2 expression in fully differentiated cells (supplemental Fig. 2, *A* and *C*). Because SCD2 depletion inhibits the increase in SCD1 expression during adipogenesis (Fig. 2*C*), perhaps the inhibition of adipogenesis is not due solely to SCD2 depletion but is dependent on a decrease in total desaturase activity. Therefore, perhaps the more profound effect of SCD2 depletion on adipogenesis is simply due to its higher expression in the preadipocyte. We, therefore, tested whether SCD1 or SCD2 are required to sustain adipocyte-specific gene expression in fully differentiated adipocytes (7 days after initiation of differentiation), when SCD1 expression is dramatically higher than SCD2 expression (supplemental Fig. 2*C*). Remarkably, real time-PCR analysis of the products of several adipocyte genes revealed that SCD2, but not SCD1, is necessary for optimal expression of the PPAR $\gamma$ -regulated genes, phosphoenolpyruvate carboxy kinase, and ACC $\beta$  in fully differentiated cells (Fig. 5*A*). However, SCD2 knockdown in these fully differentiated adipocytes only caused a minor decrease in PPAR $\gamma$  mRNA expression (Fig. 5*A*), in contrast to SCD2 depletion in cells before differentiation (Fig. 2*A*). Therefore, the expression of PPAR $\gamma$ 1 and PPAR $\gamma$ 2 protein was determined by Western blot (Fig. 5*B*). Surprisingly, the protein levels of both PPAR $\gamma$  isoforms were markedly decreased in fully differentiated adipocytes upon siRNA-mediated depletion of SCD2 and not affected by depletion of SCD1. FAS is also required for phosphoenolpyruvate carboxy kinase and ACC $\beta$  expression in fully differentiated cells, but this effect is not due to a decrease in PPAR $\gamma$  expression, since FAS depletion did not cause a sig-

nificant decrease in PPAR $\gamma$  mRNA or protein expression (Figs. 5, *A* and *B*). Thus, the maintenance of PPAR $\gamma$  protein in fully differentiated cultured adipocytes is specifically dependent on SCD2 activity, explaining the requirement of SCD2 for phosphoenolpyruvate carboxy kinase and ACC $\beta$  gene expression.

To compare the sets of adipocyte genes regulated by SCD2 depletion *versus* PPAR $\gamma$  depletion, Affymetrix Gene Chip analysis was performed in fully differentiated adipocytes electroporated with siRNA directed against PPAR $\gamma$ , SCD1, or SCD2. Fig. 6 illustrates the results of this analysis as a heat map showing the comparison of genes that change in expression with the different siRNA treatments. The *green bars* represent genes that are significantly up-regulated, and the *red bars* represent genes that are significantly down-regulated in the cells treated with siRNA *versus* scrambled nucleotide control. Not surprisingly, SCD2 depletion has a profound effect on gene expression that strongly parallels the effects of PPAR $\gamma$  depletion, whereas loss of SCD1 shows no similarity to PPAR $\gamma$  depletion in its effect on gene expression (Fig. 6). Likewise, a closer analysis of genes highly expressed in the adipocyte reveals similar changes in gene expression due to PPAR $\gamma$  and SCD2 depletion but not SCD1 depletion (supplemental Table 1). In these experiments, PPAR $\gamma$  depletion by siRNA was only about 50% (data not shown). Therefore, these results demonstrate the powerful requirement of PPAR $\gamma$  for optimal adipocyte-specific gene expression, as previously published (7). Furthermore, these results illustrate the distinct roles that the highly similar desaturases SCD1 and SCD2 fulfill in the fully differentiated adipocyte.

*SCD2 Is Required for Optimal Protein Synthesis in 3T3-L1 Adipocytes*—The reduction in PPAR $\gamma$  protein but not mRNA expression in response to SCD2 depletion in fully differentiated adipocytes may be due to a decrease in its synthesis or an increase in its degradation. Cultured adipocytes were, therefore, treated with cycloheximide to inhibit protein synthesis and determine whether PPAR $\gamma$  degradation is increased upon loss of SCD2. Using this standard method to determine the protein degradation rate in the presence of cycloheximide, PPAR $\gamma$  protein levels were assessed in adipocytes that were electroporated with scrambled siRNA or siRNA directed against SCD2. As seen in Fig. 7, the rate of loss of PPAR $\gamma$  protein is rapid upon this treatment, exhibiting a short half-life of  $\sim$ 1.5 h similar to what has been previously reported (30). However, the rate of PPAR $\gamma$  degradation is similar between control and SCD2-depleted cells, indicating no change in response to loss of SCD2. Therefore, these results confirm rapid turnover of PPAR $\gamma$  protein in adipocytes and indicate that SCD2 does not promote PPAR $\gamma$  degradation.

The results in Fig. 7 indicate that the decrease in PPAR $\gamma$  protein levels in response to the loss of SCD2 in fully differentiated adipocytes is due to decreased synthesis of PPAR $\gamma$  protein. To determine whether SCD2 is required for PPAR $\gamma$  protein synthesis, newly synthesized protein was labeled with [ $^{35}$ S]methionine/cysteine, and PPAR $\gamma$  protein was immunoprecipitated from control and SCD2-depleted cells. The radioactive signal generated from the immunoprecipitated protein indicates protein that has been newly synthe-



## Regulation of PPAR $\gamma$ Expression by SCD2

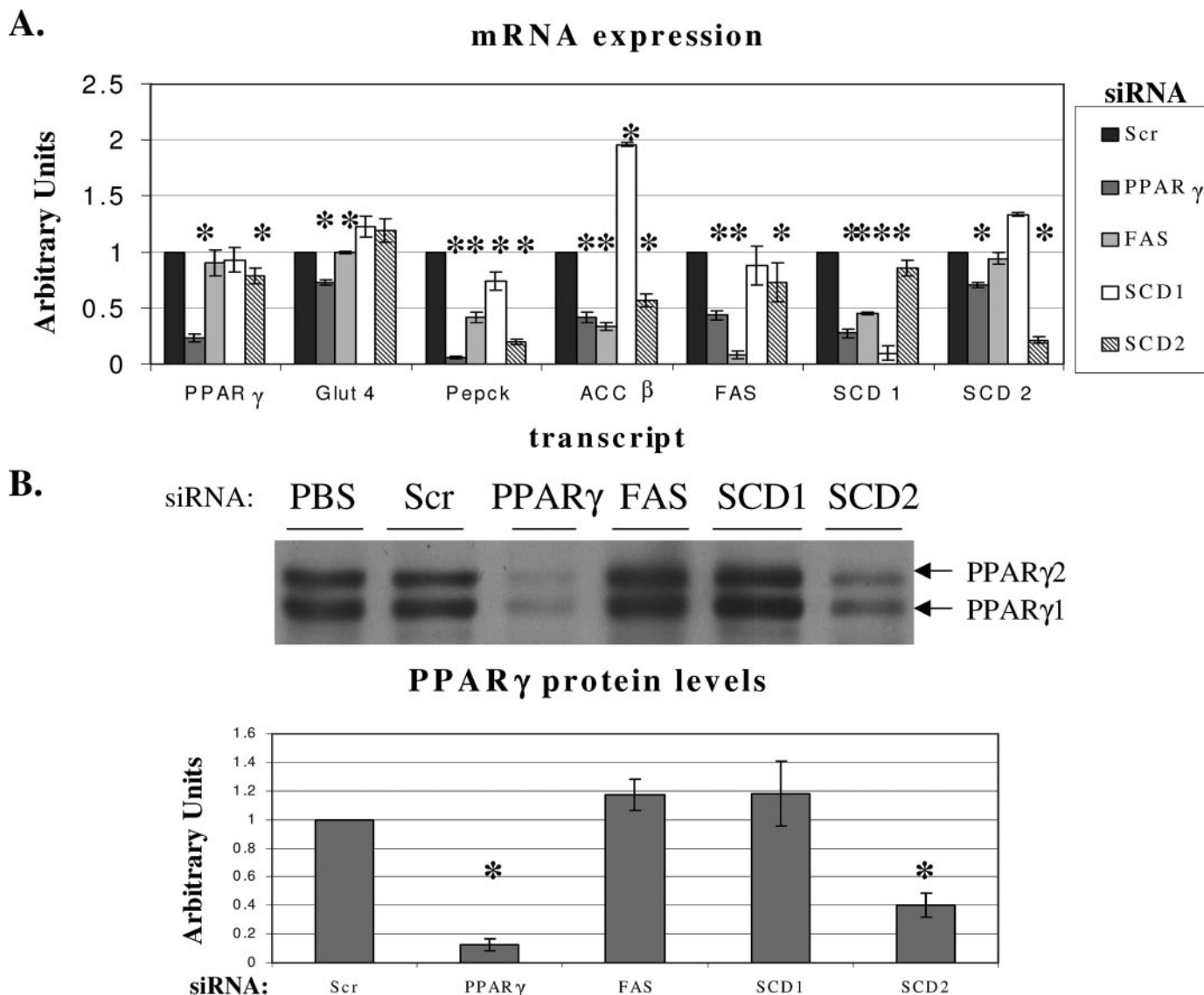


**FIGURE 5. SCD2 is required for PPAR $\gamma$  protein, but not mRNA expression, as well as the expression of the PPAR $\gamma$ -regulated genes, phosphoenolpyruvate carboxykinase, and ACC $\beta$  in fully differentiated 3T3-L1 adipocytes.** Seven days post-differentiation, adipocytes were electroporated with PBS or scrambled nucleotide as controls or siRNA against PPAR $\gamma$ , FAS, SCD1, or SCD2 transcript. After 72 h, RNA was collected to determine the expression of adipogenic markers by real time PCR using AKT1 as an internal control (A) or protein was collected to determine the expression of PPAR $\gamma$  by Western blot (B). Changes in protein expression were quantified by densitometry; the values for PPAR $\gamma$  represent both PPAR $\gamma$ 1 and PPAR $\gamma$ 2 isoforms, since both isoforms show a similar decrease. The values represent the average of three independent experiments, and the asterisk denotes a  $p$  value  $< 0.05$ . PEPCCK, phosphoenolpyruvate carboxykinase.

sized, whereas the Western blot of the immunoprecipitated protein shows the total amount of protein present. As seen in Fig. 8, newly synthesized PPAR $\gamma$ 1 and PPAR $\gamma$ 2 are reduced by ~50% in the SCD2 depleted cells, which is similar to the decrease in total protein levels (Figs. 8 and 5B). Therefore, because PPAR $\gamma$  degradation is not altered (Fig. 7), the decrease in newly synthesized protein appears to be due to a decrease in protein synthesis.

A common method to monitor the translational efficiency of a particular mRNA is by polysome profile analysis. This methodology separates monosomes from polysomes using a sucrose density gradient, which is then fractionated to generate an absorbance profile, indicating which fractions contain monosomes and polysomes. Subsequently, mRNA is isolated from each fraction to determine the degree to which

a particular mRNA associates with monosomes or polysomes. To verify that translation of PPAR $\gamma$  is indeed decreased in response to SCD2 depletion, polysome profile analysis was performed, and the distribution of PPAR $\gamma$  mRNA with monosomes and polysomes was determined. The UV absorbance at  $A_{254}$  reveals a decrease in the absorbance in the heavy polysome fractions and an increase in absorbance in the light polysome and 80 S monosome fractions in cells depleted of SCD2, suggesting that less ribosomes are associated with mRNA, and there is a global reduction in translation. Real time PCR analysis also reveals that the PPAR $\gamma$  mRNA shifts toward the lighter polysome and monosome fractions, confirming that PPAR $\gamma$  is less efficiently translated in the absence of SCD2 (Fig. 8). Therefore, the decrease in PPAR $\gamma$  protein expression is due to a

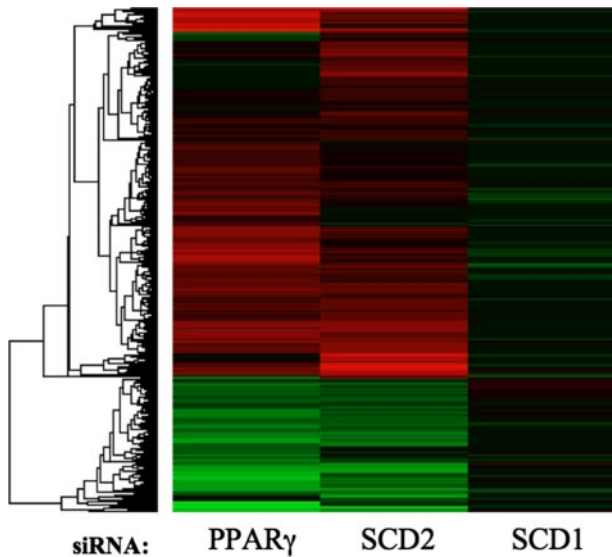


**FIGURE 6. Depletion of SCD2, but not SCD1, attenuates the expression of PPAR $\gamma$ -regulated genes.** Heat map showing the comparison of genes that change in expression with PPAR $\gamma$ , SCD2, or SCD1 depletion. Seven days post-differentiation, adipocytes were transfected with siRNA against PPAR $\gamma$ , SCD2, SCD1, or scramble nucleotide control, and RNA was collected after 72 h to perform Affymetrix GeneChip analysis. The *first column* is a comparison of scrambled nucleotide *versus* PPAR $\gamma$  depletion; the *second column* is a comparison of scrambled nucleotide *versus* SCD2 depletion; the *third column* is a comparison of scrambled nucleotide *versus* SCD1 depletion. *Green bars* represent genes that are significantly up-regulated, and *red bars* represent genes that are down-regulated ( $p < 0.05$ ).

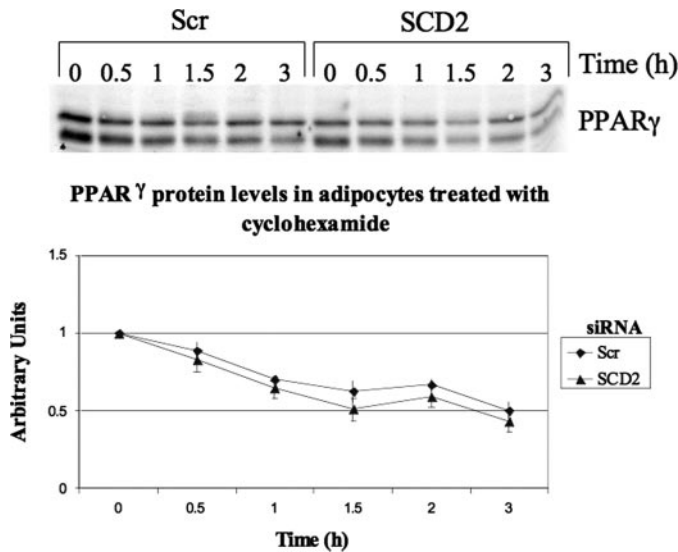


**FIGURE 7. SCD2 depletion does not enhance degradation of PPAR $\gamma$ .** Seven days post-differentiation, adipocytes were electroporated as described, and after 24 h of siRNA transfection, cells were treated with 5  $\mu$ M cycloheximide. Protein was collected at the indicated time points and analyzed by Western blot. Shown is a representative blot. Proteins were quantified by densitometry, and the 0.5–3-h time points were normalized to the time 0 time point for each condition to calculate the -fold change in time for protein turnover. The graph illustrates the average of six independent experiments.

decrease in general protein synthesis and does not specifically affect PPAR $\gamma$  translation.

## DISCUSSION

The major finding reported here is the unexpected requirement of the fatty acid desaturase isoform SCD2 for both adipo-

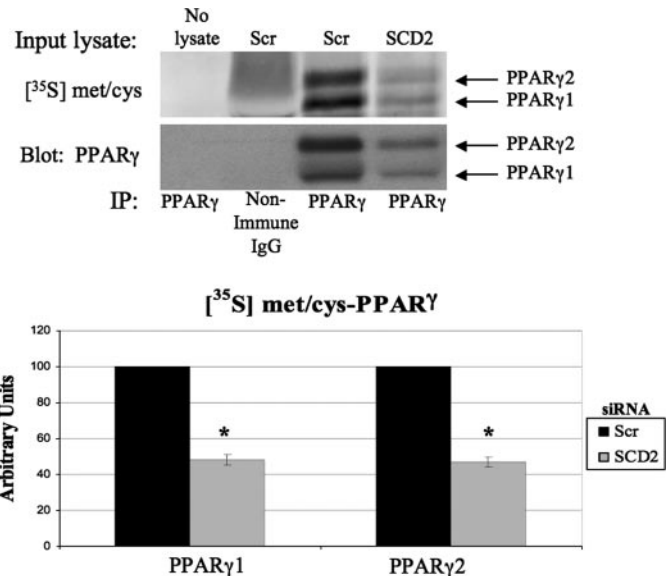


**FIGURE 8. SCD2 depletion inhibits the synthesis of PPAR $\gamma$  protein.** Seven days post-differentiation adipocytes were electroporated as described, and 72 h after siRNA transfection, cells were metabolically labeled with [<sup>35</sup>S]Met/Cys and washed several times, and protein was collected for PPAR $\gamma$  immunoprecipitation and Western blot. The radioactive signal was visualized using a PhosphorImager (Molecular Dynamics) and quantified by densitometry. Shown is a representative immunoprecipitation (IP) of PPAR $\gamma$  labeled with [<sup>35</sup>S]Met/Cys or anti-PPAR $\gamma$  antibody. The graph illustrates the average of three experiments, and the *asterisk* denotes a  $p$  value  $< 0.01$ .

genesis and the maintenance of the adipocyte phenotype in cultured 3T3-L1 cells (Figs. 2, 3, 5, and 6, and supplemental Fig. 1). SCD2 regulates adipogenesis at least in part by controlling the transcription of the nuclear receptor PPAR $\gamma$  (Fig. 2A and supplemental Fig. 1), whereas in fully differentiated adipocytes SCD2 is required for optimal protein synthesis, including PPAR $\gamma$  translation (Figs. 7–9). Thus, in 3T3-L1 preadipocytes and adipocytes, PPAR $\gamma$  protein levels are remarkably dependent on the expression levels of SCD2. Interestingly, the inhibition of adipogenesis by SCD2 depletion was not restored by the addition of the PPAR $\gamma$ -specific ligand, rosiglitazone (Figs. 2 and 3 and supplemental Fig. 1). Therefore, SCD2 does not appear to be regulating the production of a PPAR $\gamma$  ligand. Rather, these data indicate that in preadipocytes one or more unsaturated fatty acids generated by the SCD2 enzyme or a protein-protein interaction dependent on SCD2 is necessary for the normal functioning of the transcriptional machinery that drives PPAR $\gamma$  expression and also to maintain protein synthesis rates in mature adipocytes.

The surprisingly powerful effects of depleting SCD2 in cultured adipocytes suggest a special role for this enzyme in adipocyte function. We tested the effects of depleting 24 enzymes that catalyze reactions in fatty acid metabolism in our siRNA-based screen, but only FAS and SCD2 were found to be necessary for adipogenesis (Figs. 2 and 3 and supplemental Fig. 1). Mice express 4 isoforms of SCD (SCD1–4), which exhibit ~80% sequence similarity, whereas humans have two isoforms (SCD1 and SCD5) that are ~60% similar in sequence (31–33). However, all four mouse SCD isoforms are nearly 80% similar to human SCD1 (31, 32, 34, 35). Mouse SCD1 is the best characterized SCD isoform and is expressed in adipose tissue, liver,

## Regulation of PPAR $\gamma$ Expression by SCD2

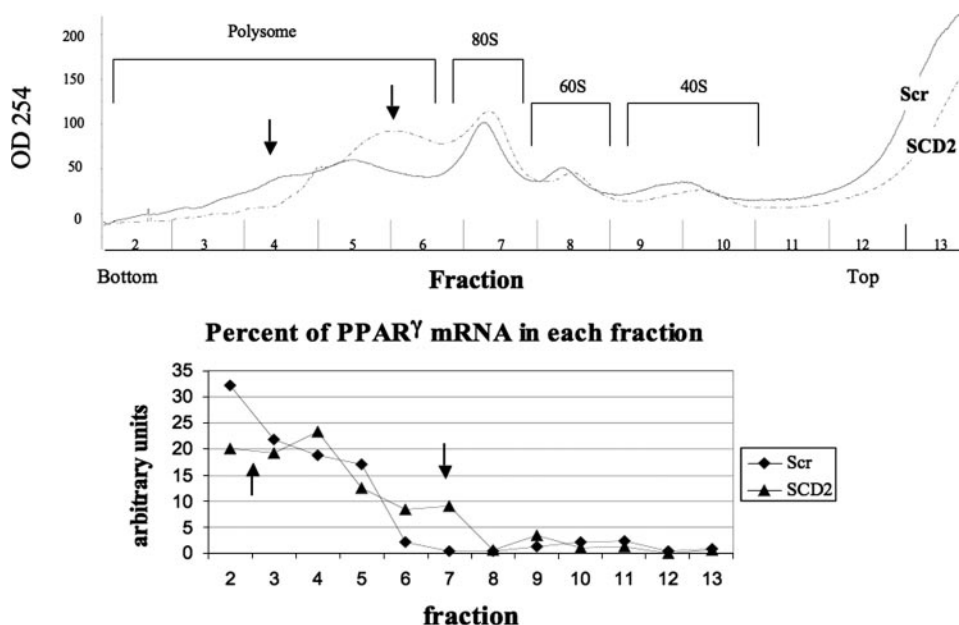


**FIGURE 9. SCD2 depletion decreases polysome association with mRNA in cultured adipocytes.** Seven days post-differentiation, adipocytes were electroporated as described, and after 24 h of siRNA transfection, cytoplasmic extracts were prepared and fractionated on a 10–50% sucrose gradient. The absorbance of each fraction was determined at  $A_{254}$ , and total RNA was extracted from fractions 2–13. PPAR $\gamma$  mRNA was quantified from equal volumes of the fractions using real time PCR and expressed as a percentage of the maximum PPAR $\gamma$  mRNA in each sample. The data shown represents one of four experiments with similar results.

muscle, and sebaceous glands, SCD2 is expressed ubiquitously, SCD3 is expressed in the harderian gland and in sebocytes in the skin, and SCD4 is expressed in the heart (31). The reason for multiple highly homologous isoforms in the mouse has remained unclear, especially since SCD1 and SCD2 apparently utilize the same substrates with the same efficiency (29). One possible explanation for the redundancy in SCD isoforms is the need for differential expression in various tissues during specific stages of development (31). However, depletion of SCD1 in fully differentiated cells did not have a major impact on adipocyte-specific gene expression despite the higher expression of SCD1 *versus* SCD2 (supplemental Fig. 2C). Therefore, despite the predicted similarity in substrate usage and common cellular localizations of the enzymes, SCD1 and SCD2 appear to have disparate cellular functions in 3T3-L1 adipocytes (29, 31, 34, 35). Interestingly, Affymetrix Gene Chip analysis reveals that when mice are put on a high fat diet, SCD2 expression increases 44-fold, whereas SCD1 expression shows little change (Table 1). These data suggest that SCD2 may also have a specific role in promoting adipogenesis *in vivo* since its expression increases during a time of increased adipogenesis (36) despite the already high expression of SCD1 (34, 37).

It should be noted that the requirement for a  $\Delta 9$ -desaturase during adipogenesis is somewhat surprising since Gomez *et al.* (38) showed that adipogenesis of 3T3-L1 cells is not affected when induced in the presence of the SCD chemical inhibitor, stercularic acid. Perhaps this discrepancy can be explained by a selectivity of the inhibitor for the highly homologous protein, SCD1, thereby preserving SCD2 activity and adipogenesis. This would be consistent with our results showing that the depletion of SCD1 did not attenuate adipogenesis. Nevertheless, our studies presented here are not the first evidence suggesting sep-

arate cellular functions of the enzymes, since SCD1 deficiency leads to skin abnormalities despite SCD2 expression in the skin (32).

PPAR $\gamma$  protein expression was found to be dramatically reduced upon SCD2 depletion in mature adipocytes (Figs. 3A and 5B), which explains why there is a decrease in the expression of many PPAR $\gamma$ -regulated genes (Fig. 5A). Furthermore, the reduction in PPAR $\gamma$  protein expression is due to a decrease in general protein synthesis and not degradation, since the turnover of PPAR $\gamma$  protein when protein synthesis is inhibited by cycloheximide is unaffected by the depletion of SCD2 (Fig. 7). Consistent with this interpretation, there is a decrease in newly synthesized PPAR $\gamma$  protein as determined by [ $^{35}$ S]methionine/cysteine labeling (Fig. 8) and in the association of actively translating ribosomes with mRNA, including PPAR $\gamma$  mRNA (Fig. 9).

Because SCD2 is required for general protein synthesis, PPAR $\gamma$  is not the only protein that is reduced in expression upon SCD2 depletion. In fact, examination of the total lysate from cells labeled with [ $^{35}$ S]methionine/cysteine shows a significant 15% decrease in newly synthesized protein from SCD2-depleted cells (data not shown). Unlike PPAR $\gamma$ , however, many proteins decrease in expression on the transcript level; conversely, many transcripts also increase in expression with SCD2 depletion (Fig. 6), which taken together makes it difficult to determine the effect of SCD2 on total protein synthesis. SCD2 depletion does result in the post-transcriptional decrease in expression of proteins other than PPAR $\gamma$ , such as AKT1 and  $\beta$  catenin. The decreased expression of these proteins also appears to be due to a decrease in translational efficiency since the association of AKT1 and  $\beta$  catenin mRNA shifts from polysomes to monosomes (data not shown). However, we have not verified that the synthesis of these proteins is decreased using [ $^{35}$ S]methionine/cysteine metabolic labeling or determined if the degradation rate of these proteins increases with SCD2 depletion; therefore, we cannot conclude that the decrease in their expression is due to a decrease in translation.

Altogether, our data indicate that unsaturated fatty acids may regulate a pathway to enhance the machinery of protein translation in adipocytes. Because oleate is a major unsaturated fatty acid product of SCD2, we tested whether exogenous addition of oleate would restore the decrease in PPAR $\gamma$  protein levels with SCD2 depletion (29, 31). However, even the addition of oleate at a concentration as high as 1 mM did not restore PPAR $\gamma$  levels (data not shown). Therefore, perhaps SCD2 is required to produce an unsaturated fatty acid other than oleate, or is required for the proper shuttling of an unsaturated fatty acid, as seen with linoleate in the SCD2 knock-out mouse (31),

or is necessary for a protein-protein interaction that regulates translation.

To our knowledge the only previously published evidence of regulation by unsaturated fatty acids of protein synthesis is by arachidonic acid or eicosapentaenoic acid. Arachidonic acid has been shown to both activate and inhibit protein translation in diverse cell systems, whereas eicosapentaenoic acid has been shown to inhibit translation initiation by inducing eIF2 $\alpha$  phosphorylation (39–41). Therefore, we examined eIF2 $\alpha$  phosphorylation in response to depletion of SCD2 but did not find a difference between SCD2-depleted and control adipocytes (data not shown). Protein synthesis can also be controlled through the protein kinases AMP-activated protein kinase and mTOR (42). An increase in AMP-activated protein kinase activity could lead to decreased peptide elongation through activation of eEF2 kinase, which then phosphorylates and inhibits eEF2, a factor that promotes protein chain elongation. Interestingly, this pathway may be regulated by unsaturated fatty acids, since SCD1 deficiency in mice leads to increased AMP-activated protein kinase activity in the liver (43). In SCD2-depleted adipocytes, we did find an approximate 80% increase in AMP-activated protein kinase phosphorylation and a small 20% increase in eEF2 phosphorylation compared with control cells (data not shown). However, these increases in AMP-activated protein kinase and eEF2 phosphorylation associated with SCD2 depletion do not appear to mediate the decrease we observe in protein synthesis, since eliminating the increase in phosphorylation of eEF2 by the dual depletion of eEF2 kinase and SCD2 did not restore PPAR $\gamma$  protein levels (data not shown). It is reported that mTOR positively regulates protein synthesis by phosphorylating and activating RS6K and 4EBP1 (44, 45). Although SCD2 depletion causes a reduction in RS6K and 4EBP1 protein levels, it does not reduce the phosphorylation of these proteins, suggesting the mTOR pathway is not affected (data not shown). Consistent with these results, inhibition of mTOR with rapamycin also decreases RS6K1 and RS6K2 activity but does not affect PPAR $\gamma$  levels (44, 46, 47). Therefore, it remains unclear how SCD2 regulates mRNA association with polyosomes, and this is an important question for future studies to address.

It will also be interesting in future studies to test whether SCD2 plays a unique role in modulating glucose homeostasis in mice. White adipose tissue is a key regulator of whole body metabolism through its ability to control glucose disposal and insulin sensitivity in peripheral tissues (1, 17). This regulation appears to be mediated by two main mechanisms (1, 17, 48), 1) storing excess fatty acids in the form of triglyceride to prevent lipotoxicity in peripheral tissues and 2) secreting insulin-sensitizing factors, such as adiponectin. PPAR $\gamma$  plays a central role in both of these processes by promoting expression of genes involved in fatty acid esterification to triglyceride (48) and the expression of adiponectin (48, 49). SCD2 may have profound influence on these processes through its regulation of PPAR $\gamma$  and adipogenesis. Unfortunately, SCD2<sup>-/-</sup> mice do not survive and can not be studied in this regard. Thus, these important questions regarding the

physiological role of SCD2 in whole body metabolism must await the generation of mouse models with tissue-specific depletion of this enzyme.

*Acknowledgments*—We thank Drs. Silvia Corvera, Heidi Tissenbaum, Stephen Doxsey, Adilson Guilherme, Joseph Virbasius, and James Ntambi for significant input into the development of this project.

## REFERENCES

- Kintscher, U., and Law, R. E. (2005) *Am. J. Physiol. Endocrinol. Metab.* **288**, 287–291
- Rosen, E. D., Sarraf, P., Troy, A. E., Bradwin, G., Moore, K., Milstone, D. S., Spiegelman, B. M., and Mortensen, R. M. (1999) *Mol. Cell* **4**, 611–617
- Rosen, E. D., Walkey, C. J., Puigserver, P., and Spiegelman, B. M. (2000) *Genes Dev.* **14**, 1293–1307
- Tang, Q. Q., Zhang, J. W., and Daniel Lane, M. (2004) *Biochem. Biophys. Res. Commun.* **319**, 235–239
- Rangwala, S. M., and Lazar, M. A. (2000) *Annu. Rev. Nutr.* **20**, 535–559
- Farmer, S. R. (2005) *Int. J. Obes. (Lond)* **29**, Suppl. 1, 13–16
- Tamori, Y., Masugi, J., Nishino, N., and Kasuga, M. (2002) *Diabetes* **51**, 2045–2055
- Camp, H. S., Chaudhry, A., and Leff, T. (2001) *Endocrinology* **142**, 3207–3213
- Gampe, R. T., Jr., Montana, V. G., Lambert, M. H., Miller, A. B., Bledsoe, R. K., Milburn, M. V., Kliewer, S. A., Willson, T. M., and Xu, H. E. (2000) *Mol. Cell* **5**, 545–555
- Mandrup, S., Sorensen, R. V., Helledie, T., Nohr, J., Baldursson, T., Gram, C., Knudsen, J., and Kristiansen, K. (1998) *J. Biol. Chem.* **273**, 23897–23903
- Bull, A. W., Steffensen, K. R., Leers, J., and Rafter, J. J. (2003) *Carcinogenesis* **24**, 1717–1722
- Huang, J. T., Welch, J. S., Ricote, M., Binder, C. J., Willson, T. M., Kelly, C., Witztum, J. L., Funk, C. D., Conrad, D., and Glass, C. K. (1999) *Nature* **400**, 378–382
- Schopfer, F. J., Lin, Y., Baker, P. R., Cui, T., Garcia-Barrio, M., Zhang, J., Chen, K., Chen, Y. E., and Freeman, B. A. (2005) *Proc. Natl. Acad. Sci. U. S. A.* **102**, 2340–2345
- Tzamelis, I., Fang, H., Ollero, M., Shi, H., Hamm, J. K., Kievit, P., Hollenberg, A. N., and Flier, J. S. (2004) *J. Biol. Chem.* **279**, 36093–36102
- Baker, P. R., Lin, Y., Schopfer, F. J., Woodcock, S. R., Groeger, A. L., Batthyany, C., Sweeney, S., Long, M. H., Iles, K. E., Baker, L. M., Branchaud, B. P., Chen, Y. E., and Freeman, B. A. (2005) *J. Biol. Chem.* **280**, 42464–42475
- Forman, B. M., Tontonoz, P., Chen, J., Brun, R. P., Spiegelman, B. M., and Evans, R. M. (1995) *Cell* **83**, 803–812
- Kersten, S. (2002) *Eur. J. Pharmacol.* **440**, 223–234
- Stewart, W. C., Baugh, J. E., Jr., Floyd, Z. E., and Stephens, J. M. (2004) *Biochem. Biophys. Res. Commun.* **324**, 355–359
- Kim, J. B., Wright, H. M., Wright, M., and Spiegelman, B. M. (1998) *Proc. Natl. Acad. Sci. U. S. A.* **95**, 4333–4337
- Levert, K. L., Waldrop, G. L., and Stephens, J. M. (2002) *J. Biol. Chem.* **277**, 16347–16350
- Schmid, B., Rippmann, J. F., Tadayon, M., and Hamilton, B. S. (2005) *Biochem. Biophys. Res. Commun.* **328**, 1073–1082
- Jiang, Z. Y., Zhou, Q. L., Coleman, K. A., Chouinard, M., Boese, Q., and Czech, M. P. (2003) *Proc. Natl. Acad. Sci. U. S. A.* **100**, 7569–7574
- Wilson-Fritch, L., Burkart, A., Bell, G., Mendelson, K., Leszyk, J., Nicoloso, S., Czech, M., and Corvera, S. (2003) *Mol. Cell. Biol.* **23**, 1085–1094
- Tang, X., Guilherme, A., Chakladar, A., Powelka, A. M., Konda, S., Virbasius, J. V., Nicoloso, S. M., Straubhaar, J., and Czech, M. P. (2006) *Proc. Natl. Acad. Sci. U. S. A.* **103**, 2087–2092
- Wang, X., and Seed, B. (2003) *Nucleic Acids Res.* **31**, 1–8
- Nottrott, S., Simard, M. J., and Richter, J. D. (2006) *Nat. Struct. Mol. Biol.* **13**, 1108–1114
- Lee, M. J., Yang, R. Z., Gong, D. W., and Fried, S. K. (2007) *J. Biol. Chem.* **282**, 72–80
- Taha, C., Liu, Z., Jin, J., Al-Hasani, H., Sonenberg, N., and Klip, A. (1999)

## Regulation of PPAR $\gamma$ Expression by SCD2

- J. Biol. Chem.* **274**, 33085–33091
29. Miyazaki, M., Bruggink, S. M., and Ntambi, J. M. (2006) *J. Lipid Res.* **47**, 700–704
30. Floyd, Z. E., and Stephens, J. M. (2002) *J. Biol. Chem.* **277**, 4062–4068
31. Miyazaki, M., Dobrzyn, A., Elias, P. M., and Ntambi, J. M. (2005) *Proc. Natl. Acad. Sci. U. S. A.* **102**, 12501–12506
32. Miyazaki, M., Man, W. C., and Ntambi, J. M. (2001) *J. Nutr.* **131**, 2260–2268
33. Zhang, S., Yang, Y., and Shi, Y. (2005) *Biochem. J.* **388**, 135–142
34. Ntambi, J. M., and Miyazaki, M. (2004) *Prog. Lipid Res.* **43**, 91–104
35. Man, W. C., Miyazaki, M., Chu, K., and Ntambi, J. M. (2006) *J. Biol. Chem.* **281**, 1251–1260
36. Aslan, H., Altunkaynak, B. Z., Altunkaynak, M. E., Vuraler, O., Kaplan, S., and Unal, B. (2006) *Obes. Surg.* **16**, 1526–1534
37. Ntambi, J. M., Miyazaki, M., Stoehr, J. P., Lan, H., Kendzioriski, C. M., Yandell, B. S., Song, Y., Cohen, P., Friedman, J. M., and Attie, A. D. (2002) *Proc. Natl. Acad. Sci. U. S. A.* **99**, 11482–11486
38. Gomez, F. E., Bauman, D. E., Ntambi, J. M., and Fox, B. G. (2003) *Biochem. Biophys. Res. Commun.* **300**, 316–326
39. Rotman, E. I., Brostrom, M. A., and Brostrom, C. O. (1992) *Biochem. J.* **282**, 487–494
40. Aktas, H., and Halperin, J. A. (2004) *J. Nutr.* **134**, 2487–2491
41. Neeli, I., Yellaturu, C. R., and Rao, G. N. (2003) *Biochem. Biophys. Res. Commun.* **309**, 755–761
42. Meric, F., and Hunt, K. K. (2002) *Mol. Cancer Ther.* **1**, 971–979
43. Dobrzyn, P., Dobrzyn, A., Miyazaki, M., Cohen, P., Asilmaz, E., Hardie, D. G., Friedman, J. M., and Ntambi, J. M. (2004) *Proc. Natl. Acad. Sci. U. S. A.* **101**, 6409–6414
44. Dufner, A., and Thomas, G. (1999) *Exp. Cell Res.* **253**, 100–109
45. Tsukiyama-Kohara, K., Poulin, F., Kohara, M., DeMaria, C. T., Cheng, A., Wu, Z., Gingras, A. C., Katsume, A., Elchebly, M., Spiegelman, B. M., Harper, M. E., Tremblay, M. L., and Sonenberg, N. (2001) *Nat. Med.* **7**, 1128–1132
46. Pende, M., Um, S. H., Mieulet, V., Sticker, M., Goss, V. L., Mestan, J., Mueller, M., Fumagalli, S., Kozma, S. C., and Thomas, G. (2004) *Mol. Cell. Biol.* **24**, 3112–3124
47. Kim, J. E., and Chen, J. (2004) *Diabetes* **53**, 2748–2756
48. Ferre, P. (2004) *Diabetes* **53**, Suppl. 1, 43–50
49. Gustafson, B., Jack, M. M., Cushman, S. W., and Smith, U. (2003) *Biochem. Biophys. Res. Commun.* **308**, 933–939
50. Livak, K. J., and Schmittgen, T. D. (2001) *Methods* **25**, 402–408